Automatica 78 (2017) 333–340

Contents lists available at ScienceDirect

Automatica

journal homepage: www.elsevier.com/locate/automatica

Brief paper

A new framework for solving fractional optimal control problems using fractional pseudospectral methods☆

Xiaojun Tang [a,1], Yang Shi [b], Li-Lian Wang [c]

[a] School of Aeronautics, Northwestern Polytechnical University, Xi'an, Shaanxi 710072, China
[b] Department of Mechanical Engineering, University of Victoria, Victoria, B.C. V8W 3P6, Canada
[c] School of Physical and Mathematical Sciences, Nanyang Technological University, 637371, Singapore

ARTICLE INFO

Article history:
Received 20 November 2015
Received in revised form
23 November 2016
Accepted 23 November 2016

Keywords:
Optimal control
Pseudospectral methods
Equivalence

ABSTRACT

The main purpose of this work is to provide new fractional pseudospectral methods for solving fractional optimal control problems (FOCPs). We develop differential and integral fractional pseudospectral methods and prove the equivalence between them from the distinctive perspective of *Caputo fractional Birkhoff interpolation*. As a result, the present work establishes a new unified framework for solving fractional optimal control problems using fractional pseudospectral methods, which can be viewed as an extension of existing frameworks. Furthermore, we provide exact, efficient, and stable approaches to compute the associated fractional pseudospectral differentiation/integration matrices even at millions of Jacobi-type points. Numerical results on two benchmark FOCPs including a fractional bang–bang problem demonstrate the performance of the proposed methods.

1. Introduction

Fractional optimal control problems (FOCPs) can be regarded as a generalization of classical integer optimal control problems (IOCPs) in the sense that the dynamics are described by fractional differential equations (Agrawal, 2004). There are various definitions of fractional derivatives and the two most important types are the Riemann–Liouville derivatives and the Caputo derivatives. It is noteworthy here that in distinct contrast with the integer derivatives (which are locally defined in the epsilon neighborhood of a chosen point), the fractional derivatives are nonlocal in nature as they are globally defined by a definite fractional integral over a domain. Moreover, the fractional derivatives involve singular kernel/weight functions, and the solutions of fractional differential equations are usually singular near the boundaries of the domain (Chen, Shen, & Wang, 2016). More background information on the fractional calculus can be found in Oldham and Spanier (2006) and Sabatier, Agrawal, and Tenreiro Machado (2007).

Because of the complexity of most applications, FOCPs/IOCPs are often solved numerically. In recent years, a class of numerical methods called pseudospectral methods (Elnagar, Kazemi, & Razzaghi, 1995; Fahroo & Ross, 2001; Benson, Huntington, Thorvaldsen, & Rao, 2006; Huntington, 2007; Garg et al., 2010, 2011; Francolin, Benson, Hager, & Rao, 2015) has become increasingly popular in the numerical solution of IOCPs. The basic principle of pseudospectral methods is to approximate the state using a set of basis functions and discretize the dynamic constraints using collocation at a specified set of points. As a result, a continuous optimal control problem is transcribed to a finite-dimensional nonlinear programming problem (NLP) which is then solved using well-known optimization software such as SNOPT (Gill, Murray, & Saunders, 2005) and IPOPT (Biegler & Zavala, 2009). The basis functions are typically Lagrange interpolating polynomials and the collocation points are usually chosen based on Gaussian-type quadrature rules. Basically there are two primary implementation forms for pseudospectral methods: differential and integral. Although differential and integral pseudospectral methods are quite different, recent work (Tang, Liu, & Hu, 2016) has shown that they are equivalent for collocation at the Jacobi–Gauss (JG) and flipped Jacobi–Gauss–Radau (FJGR) points. Inspired by the aforementioned *global* property of the fractional derivatives and the fact of IOCPs being special cases of FOCPs, the first author

☆ The material in this paper was not presented at any conference. This paper was recommended for publication in revised form by Associate Editor Akira Kojima under the direction of Editor Ian R. Petersen.

E-mail addresses: nputxj@nwpu.edu.cn (X. Tang), yshi@uvic.ca (Y. Shi), lilian@ntu.edu.sg (L.-L. Wang).

[1] Fax: +86 29 88492344.

http://dx.doi.org/10.1016/j.automatica.2016.12.022
0005-1098/

has recently proposed the notion of fractional pseudospectral integration matrices (FPIMs) and developed integral fractional pseudospectral methods for solving FOCPs (Tang, Liu, & Wang, 2015). However, to the best of our knowledge, differential fractional pseudospectral methods for solving FOCPs have not yet received attention. Moreover, a relevant question that comes along is: does the equivalence between classical pseudospectral methods (Tang et al., 2016) still hold for fractional pseudospectral methods?

The aim of this paper is to develop new fractional pseudospectral methods and to prove the equivalence between them via a suitable Birkhoff interpolation. The present work is strikingly different from our previous work (Tang et al., 2015, 2016) in the sense of pseudospectral scheme and Birkhoff interpolation, and establishes a new unified framework for solving fractional optimal control problems using fractional pseudospectral methods. Specifically, the main contributions of this work are as follows:

(1) We propose the notion of fractional pseudospectral differentiation matrices (FPDMs) and develop differential fractional pseudospectral methods for solving FOCPs. Moreover, we propose the notion of ε-FPIMs by employing the basis of weighted Lagrange interpolating functions (Weideman & Reddy, 2000).
(2) We take a distinctive route to prove the equivalence between the proposed fractional pseudospectral methods from the perspective of *Caputo fractional Birkhoff interpolation*.
(3) We provide exact, efficient, and stable approaches to compute FPDMs/ε-FPIMs even at millions of Jacobi-type points.
(4) We extend the framework of Garg et al. (2010) to fractional pseudospectral methods with collocation at the Jacobi-type points, and that of Tang et al. (2015) to containing differential fractional pseudospectral methods.

The rest of this paper is organized as follows. In Section 2, some preliminaries are presented for subsequent developments. In Section 3, the definitions and computation of FPDMs are presented. This is followed by the definitions and computation of ε-FPIMs in Section 4. The detailed implementation of differential fractional pseudospectral methods is provided in Section 5. In Section 6, the equivalence mentioned above is proved by using the Caputo fractional Birkhoff interpolation. In Section 7, some comments on fractional pseudospectral methods are made. Numerical results on two benchmark FOCPs are shown in Section 8. Finally, Section 9 is for some concluding remarks.

2. Some preliminaries

In this section, we present the definitions of the Riemann–Liouville fractional integrals and the Caputo fractional derivatives.

Definition 1 (*Kilbas, Srivastava, & Trujillo, 2006*)**.** The left and right Riemann–Liouville fractional integrals of real order $\gamma \geq 0$ of a function $h(t), t \in [t_0, t_f]$ are defined, respectively, as

$$ {}_{t_0}\mathcal{I}_t^{\gamma} h(t) \triangleq \begin{cases} \dfrac{1}{\Gamma(\gamma)} \displaystyle\int_{t_0}^{t} (t-s)^{\gamma-1} h(s)\,\mathrm{d}s, & \gamma > 0 \\ h(t), & \gamma = 0, \end{cases} \tag{1a} $$

$$ {}_{t}\mathcal{I}_{t_f}^{\gamma} h(t) \triangleq \begin{cases} \dfrac{1}{\Gamma(\gamma)} \displaystyle\int_{t}^{t_f} (s-t)^{\gamma-1} h(s)\,\mathrm{d}s, & \gamma > 0 \\ h(t), & \gamma = 0, \end{cases} \tag{1b} $$

where $\Gamma(\cdot)$ is the Gamma function. It is noteworthy here that for $\gamma \in \mathbb{N}$, the fractional integrals coincide with the usual iterated integrals due to the well-known Cauchy's integral formula.

Definition 2 (*Kilbas et al., 2006*)**.** The left and right Caputo fractional derivatives of real order $\gamma \in (n-1, n]$, $n = \lceil \gamma \rceil \in \mathbb{N}$ of a function $h(t) \in AC^n[t_0, t_f]$ are defined, respectively, as

$$ {}_{t_0}^{C}\mathcal{D}_t^{\gamma} h(t) \triangleq {}_{t_0}\mathcal{I}_t^{n-\gamma} \left(\frac{\mathrm{d}^n}{\mathrm{d}t^n} h(t) \right), \tag{2a} $$

$$ {}_{t}^{C}\mathcal{D}_{t_f}^{\gamma} h(t) \triangleq (-1)^n {}_{t}\mathcal{I}_{t_f}^{n-\gamma} \left(\frac{\mathrm{d}^n}{\mathrm{d}t^n} h(t) \right), \tag{2b} $$

where $\lceil \gamma \rceil$ denotes the smallest integer greater than or equal to γ. In particular, we have ${}_{t_0}^{C}\mathcal{D}_t^0 h(t) = {}_{t}^{C}\mathcal{D}_{t_f}^0 h(t) = h(t)$.

3. Definitions and computation of FPDMs

In this section, the definitions and computation of FPDMs are presented.

3.1. Definitions of FPDMs

Definition 3. The left and right FPDMs of real order $\gamma \in (0, 1]$ for the JG points of $\{\tau_i \in (-1, +1)\}_{i=1}^{N}$ with $-1 = \tau_0 < \tau_1 < \cdots < \tau_{N+1} = +1$ are defined, respectively, as

$$ \begin{aligned} {}_{-1}^{\tau}\boldsymbol{D}_{ki}^{\gamma} &\triangleq {}_{-1}^{C}\mathcal{D}_{\tau_k}^{\gamma} \mathcal{L}_i^{\star}(\tau) \\ &= {}_{-1}\mathcal{I}_{\tau_k}^{1-\gamma} \dot{\mathcal{L}}_i^{\star}(\tau), \\ &\quad (k = 1, 2, \ldots, N,\ i = 0, 1, \ldots, N), \end{aligned} \tag{3a} $$

$$ \begin{aligned} {}_{\tau}^{1}\boldsymbol{D}_{ki}^{\gamma} &\triangleq {}_{\tau_k}^{C}\mathcal{D}_{1}^{\gamma} \mathcal{L}_i^{\dagger}(\tau) \\ &= -\left({}_{\tau_k}\mathcal{I}_{1}^{1-\gamma} \dot{\mathcal{L}}_i^{\dagger}(\tau) \right), \\ &\quad (k = 1, 2, \ldots, N,\ i = 1, 2, \ldots, N+1), \end{aligned} \tag{3b} $$

where $\{\mathcal{L}_i^{\star}(\tau) \in \mathcal{P}_N\}_{i=0}^{N}$ and $\{\mathcal{L}_i^{\dagger}(\tau) \in \mathcal{P}_N\}_{i=1}^{N+1}$ are the Nth-order Lagrange interpolating polynomials associated with the interpolating points $\{\tau_i\}_{i=0}^{N}$ and $\{\tau_i\}_{i=1}^{N+1}$, respectively, defined as

$$ \mathcal{L}_i^{\star}(\tau) \triangleq \prod_{j=0, j\neq i}^{N} \frac{\tau - \tau_j}{\tau_i - \tau_j}, \quad i = 0, 1, \ldots, N, \tag{4a} $$

$$ \mathcal{L}_i^{\dagger}(\tau) \triangleq \prod_{j=1, j\neq i}^{N+1} \frac{\tau - \tau_j}{\tau_i - \tau_j}, \quad i = 1, 2, \ldots, N+1, \tag{4b} $$

where $\mathcal{P}_N$ denotes the set of all polynomials of degree $\leq N$. Moreover, let $\{\mathcal{L}_i(\tau) \in \mathcal{P}_{N-1}\}_{i=1}^{N}$ be the $(N-1)$th-order Lagrange interpolating polynomials associated with the interpolating points $\{\tau_i\}_{i=1}^{N}$, defined as

$$ \mathcal{L}_i(\tau) \triangleq \prod_{j=1, j\neq i}^{N} \frac{\tau - \tau_j}{\tau_i - \tau_j}, \quad i = 1, 2, \ldots, N. \tag{5} $$

Then from Eqs. (4) and (5), we have

$$ \mathcal{L}_i^{\star}(\tau) = \frac{\tau - \tau_0}{\tau_i - \tau_0} \cdot \mathcal{L}_i(\tau), \quad i = 1, 2, \ldots, N, \tag{6a} $$

$$ \mathcal{L}_i^{\dagger}(\tau) = \frac{\tau_{N+1} - \tau}{\tau_{N+1} - \tau_i} \cdot \mathcal{L}_i(\tau), \quad i = 1, 2, \ldots, N. \tag{6b} $$

Note that Eq. (6a) has already been given in Tang et al. (2016, Eq. (11)).

Definition 4. The left FPDM of real order $\gamma \in (0, 1]$ for the FJGR points of $\{\hat{\tau}_i \in (-1, +1]\}_{i=1}^{N}$ with $-1 = \hat{\tau}_0 < \hat{\tau}_1 < \cdots < \hat{\tau}_N = +1$, and the right FPDM of real order $\gamma \in (0, 1]$ for the

Jacobi–Gauss–Radau (JGR) points of $\{\check{\tau}_i \in [-1,+1)\}_{i=1}^{N}$ with $-1=\check{\tau}_1<\check{\tau}_2<\cdots<\check{\tau}_{N+1}=+1$ are defined, respectively, as

$$\begin{aligned}{}_{-1}^{\tau}\hat{\boldsymbol{D}}_{ki}^{\gamma} &\triangleq {}_{-1}^{C}\mathcal{D}_{\hat{\tau}_k}^{\gamma}\hat{\mathcal{L}}_i^{\star}(\tau)\\ &= {}_{-1}\mathcal{I}_{\hat{\tau}_k}^{1-\gamma}\dot{\hat{\mathcal{L}}}_i^{\star}(\tau),\\ &\quad (k=1,2,\ldots,N,\ i=0,1,\ldots,N),\end{aligned}\tag{7a}$$

$$\begin{aligned}{}_{\tau}^{1}\check{\boldsymbol{D}}_{ki}^{\gamma} &\triangleq {}_{\check{\tau}_k}^{C}\mathcal{D}_{1}^{\gamma}\check{\mathcal{L}}_i^{\dagger}(\tau)\\ &= -\left({}_{\check{\tau}_k}\mathcal{I}_{1}^{1-\gamma}\dot{\check{\mathcal{L}}}_i^{\dagger}(\tau)\right),\\ &\quad (k=1,2,\ldots,N,\ i=1,2,\ldots,N+1),\end{aligned}\tag{7b}$$

where $\{\hat{\mathcal{L}}_i^{\star}(\tau)\in\mathcal{P}_N\}_{i=0}^{N}$ and $\{\check{\mathcal{L}}_i^{\dagger}(\tau)\in\mathcal{P}_N\}_{i=1}^{N+1}$ are defined, respectively, in Eqs. (4a) and (4b) with the corresponding interpolating points being $\{\hat{\tau}_i\}_{i=0}^{N}$ and $\{\check{\tau}_i\}_{i=1}^{N+1}$.

3.2. Computation of FPDMs

It can be seen from the definitions of FPDMs and FPIMs (Tang et al., 2015) that there is no essential difference between them. Therefore, we can take a similar approach to compute FPDMs.

We present the main results in the following two theorems, which give the general formulas to compute the left and right FPDMs for the Jacobi-type points.

Theorem 5. *Let $\{\tilde{\sigma}_m,\tilde{\omega}_m\}_{m=1}^{\lceil N/2\rceil}$ be the set of JG points and quadrature weights with respect to the Jacobi weight function $\omega^{(-\gamma,0)}(\tau)=(1-\tau)^{-\gamma}$. Then, the left FPDM of Eq. (3a) for $\gamma\in(0,1)$ can be computed exactly as*

$${}_{-1}^{\tau}\boldsymbol{D}_{ki}^{\gamma}=\begin{cases}-\sum_{j=1}^{N}{}_{-1}^{\tau}\boldsymbol{D}_{kj}^{\gamma}, & i=0\\ \dfrac{1}{\Gamma(1-\gamma)}\left(\dfrac{\tau_k+1}{2}\right)^{1-\gamma}\displaystyle\sum_{m=1}^{\lceil N/2\rceil}\tilde{\omega}_m & \\ \quad\cdot\left(\displaystyle\sum_{r=1}^{N}{}_{-1}^{\tau}\boldsymbol{D}_{ri}^{1}\cdot\mathcal{L}_r(\tilde{\sigma}_m;-1,\tau_k)\right), & i\neq 0,\end{cases}\tag{8}$$

where the computation of ${}_{-1}^{\tau}\boldsymbol{D}_{ri}^{1}$ (which corresponds to ${}_{-1}^{\tau}\boldsymbol{D}_{ri}^{\gamma}$ with $\gamma=1$) follows straightforwardly from Tang et al. (2016, Theorem 4) as

$${}_{-1}^{\tau}\boldsymbol{D}_{ri}^{1}=\dot{\mathcal{L}}_i^{\star}(\tau_r)=\boldsymbol{D}_{ri}^{\star}\tag{9a}$$

$$=\begin{cases}-\sum_{j=1}^{N}{}_{-1}^{\tau}\boldsymbol{D}_{rj}^{1}, & i=0\\ \dfrac{\delta_{ri}+(\tau_r-\tau_0)\boldsymbol{D}_{ri}}{\tau_i-\tau_0}, & i\neq 0,\end{cases}\tag{9b}$$

where δ_{ri} is the Kronecker delta and $\boldsymbol{D}_{ri}$ can be computed efficiently and stably as (Berrut & Trefethen, 2004)

$$\boldsymbol{D}_{ri}\triangleq\dot{\mathcal{L}}_i(\tau_r),\quad r,i=1,2,\ldots,N\tag{10a}$$

$$=\begin{cases}\dfrac{\xi_i/\xi_r}{\tau_r-\tau_i}, & r\neq i\\ -\displaystyle\sum_{j=1,j\neq r}^{N}\boldsymbol{D}_{rj}, & r=i,\end{cases}\tag{10b}$$

where $\{\xi_i\}_{i=1}^{N}$ are the barycentric weights for the JG points and their efficient and stable calculation is given in Wang, Huybrechs, and Vandewalle (2014) and Tang et al. (2015). The same result also holds for the FJGR points.

Proof. It follows from Eq. (3a) and Tang et al. (2015, Theorem 9) that

$${}_{-1}^{\tau}\boldsymbol{D}_{ki}^{\gamma}=\frac{1}{\Gamma(1-\gamma)}\left(\frac{\tau_k+1}{2}\right)^{1-\gamma}\sum_{m=1}^{\lceil N/2\rceil}\tilde{\omega}_m\dot{\mathcal{L}}_i^{\star}(\tilde{\sigma}_m;-1,\tau_k).\tag{11}$$

Recalling that $\dot{\mathcal{L}}_i^{\star}(\tau)\in\mathcal{P}_{N-1}$, and thus, it can be represented using the Lagrange interpolation as

$$\begin{aligned}\dot{\mathcal{L}}_i^{\star}(\tau) &= \sum_{r=1}^{N}\dot{\mathcal{L}}_i^{\star}(\tau_r)\cdot\mathcal{L}_r(\tau)\\ &= \sum_{r=1}^{N}{}_{-1}^{\tau}\boldsymbol{D}_{ri}^{1}\cdot\mathcal{L}_r(\tau).\end{aligned}\tag{12}$$

Combining Eqs. (11) and (12) leads to the second identity of Eq. (8). The first identity of Eq. (8) results from the fact that $0={}_{-1}^{C}\mathcal{D}_{\tau_k}^{\gamma}1=\sum_{i=0}^{N}{}_{-1}^{\tau}\boldsymbol{D}_{ki}^{\gamma}$, $k=1,2,\ldots,N$. □

Theorem 6. *Let $\{\check{\sigma}_m,\check{\omega}_m\}_{m=1}^{\lceil N/2\rceil}$ be the set of JG points and quadrature weights with respect to the Jacobi weight function $\omega^{(0,-\gamma)}(\tau)=(1+\tau)^{-\gamma}$. Then, the right FPDM of Eq. (3b) for $\gamma\in(0,1)$ can be computed exactly as*

$${}_{\tau}^{1}\boldsymbol{D}_{ki}^{\gamma}=\begin{cases}\dfrac{1}{\Gamma(1-\gamma)}\left(\dfrac{1-\tau_k}{2}\right)^{1-\gamma}\displaystyle\sum_{m=1}^{\lceil N/2\rceil}\check{\omega}_m & \\ \quad\cdot\left(\displaystyle\sum_{r=1}^{N}{}_{\tau}^{1}\boldsymbol{D}_{ri}^{1}\cdot\mathcal{L}_r(\check{\sigma}_m;\tau_k,1)\right), & i\neq N+1\\ -\displaystyle\sum_{j=1}^{N}{}_{\tau}^{1}\boldsymbol{D}_{kj}^{\gamma}, & i=N+1,\end{cases}\tag{13}$$

where ${}_{\tau}^{1}\boldsymbol{D}_{ri}^{1}$ (which corresponds to ${}_{\tau}^{1}\boldsymbol{D}_{ri}^{\gamma}$ with $\gamma=1$) can be easily obtained as (see Appendix)

$${}_{\tau}^{1}\boldsymbol{D}_{ri}^{1}=-\dot{\mathcal{L}}_i^{\dagger}(\tau_r)\tag{14a}$$

$$=\begin{cases}\dfrac{\delta_{ri}-(\tau_{N+1}-\tau_r)\boldsymbol{D}_{ri}}{\tau_{N+1}-\tau_i}, & i\neq N+1\\ -\displaystyle\sum_{j=1}^{N}{}_{\tau}^{1}\boldsymbol{D}_{rj}^{1}, & i=N+1.\end{cases}\tag{14b}$$

The same result also holds for the JGR points.

Proof. The proof is similar to that of Theorem 5, and thus, is omitted here for avoiding repetition. □

4. Definitions and computation of ε-FPIMs

In this section, the definitions and computation of ε-FPIMs are presented.

4.1. Definitions of ε-FPIMs

Definition 7. The left and right ε-FPIMs of real order $\gamma\in(0,1]$ for the JG points of $\{\tau_i\in(-1,+1)\}_{i=1}^{N}$ with $-1=\tau_0<\tau_1<\cdots<\tau_{N+1}=+1$ are defined, respectively, as

$$\begin{aligned}{}_{-1}^{\tau}\boldsymbol{I}_{ki}^{\gamma_\varepsilon} &\triangleq {}_{-1}\mathcal{I}_{\tau_k}^{\gamma}\mathcal{L}_i^{\grave{\varepsilon}}(\tau),\\ &\quad (k=1,2,\ldots,N+1,\ i=1,2,\ldots,N),\end{aligned}\tag{15a}$$

$$\begin{aligned}{}_{\tau}^{1}\boldsymbol{I}_{ki}^{\gamma_\varepsilon} &\triangleq {}_{\tau_k}\mathcal{I}_{1}^{\gamma}\mathcal{L}_i^{\acute{\varepsilon}}(\tau),\\ &\quad (k=0,1,\ldots,N,\ i=1,2,\ldots,N),\end{aligned}\tag{15b}$$

where $\mathcal{L}_i^{\grave{\varepsilon}}(\tau)$ and $\mathcal{L}_i^{\acute{\varepsilon}}(\tau)$ are the weighted Lagrange interpolating functions (Weideman & Reddy, 2000) associated with the weight

functions $\grave{\varepsilon}(\tau) = (\tau+1)^{1-\gamma}$ and $\acute{\varepsilon}(\tau) = (1-\tau)^{1-\gamma}$, respectively, defined as

$$\mathcal{L}_i^{\grave{\varepsilon}}(\tau) \triangleq \frac{\grave{\varepsilon}(\tau)}{\grave{\varepsilon}(\tau_i)}\mathcal{L}_i(\tau) = \frac{(\tau+1)^{1-\gamma}\mathcal{L}_i(\tau)}{(\tau_i+1)^{1-\gamma}}, \quad i=1,2,\ldots,N, \tag{16a}$$

$$\mathcal{L}_i^{\acute{\varepsilon}}(\tau) \triangleq \frac{\acute{\varepsilon}(\tau)}{\acute{\varepsilon}(\tau_i)}\mathcal{L}_i(\tau) = \frac{(1-\tau)^{1-\gamma}\mathcal{L}_i(\tau)}{(1-\tau_i)^{1-\gamma}}, \quad i=1,2,\ldots,N, \tag{16b}$$

where $\{\mathcal{L}_i(\tau)\}_{i=1}^N$ are defined in Eq. (5).

Definition 8. The left ε-FPIM of real order $\gamma \in (0,1]$ for the FJGR points of $\{\hat{\tau}_i \in (-1,+1]\}_{i=1}^N$ with $-1=\hat{\tau}_0<\hat{\tau}_1<\cdots<\hat{\tau}_N=+1$, and the right ε-FPIM of real order $\gamma\in(0,1]$ for the JGR points of $\{\check{\tau}_i\in[-1,+1)\}_{i=1}^N$ with $-1=\check{\tau}_1<\check{\tau}_2<\cdots<\check{\tau}_{N+1}=+1$ are defined, respectively, as

$${}_{-1}^{\tau}\hat{\boldsymbol{I}}_{ki}^{\gamma_{\grave{\varepsilon}}} \triangleq {}_{-1}\mathcal{I}_{\hat{\tau}_k}^{\gamma}\hat{\mathcal{L}}_i^{\grave{\varepsilon}}(\tau), \quad k,i=1,2,\ldots,N, \tag{17a}$$

$${}_{\tau}^{1}\check{\boldsymbol{I}}_{ki}^{\gamma_{\acute{\varepsilon}}} \triangleq {}_{\check{\tau}_k}\mathcal{I}_{1}^{\gamma}\check{\mathcal{L}}_i^{\acute{\varepsilon}}(\tau), \quad k,i=1,2,\ldots,N, \tag{17b}$$

where $\{\hat{\mathcal{L}}_i^{\grave{\varepsilon}}(\tau)\}_{i=1}^N$ and $\{\check{\mathcal{L}}_i^{\acute{\varepsilon}}(\tau)\}_{i=1}^N$ are defined, respectively, in Eqs. (16a) and (16b) with the corresponding interpolating points being $\{\hat{\tau}_i\}_{i=1}^N$ and $\{\check{\tau}_i\}_{i=1}^N$.

Remark 9. It is easy to see that ε-FPIMs are fundamentally different from FPIMs (Tang et al., 2015) in the interpolating basis functions. More precisely, the weighted Lagrange interpolating functions (Weideman & Reddy, 2000) are adopted in ε-FPIMs while the Lagrange interpolating polynomials were used in FPIMs (Tang et al., 2015).

Remark 10. The new basis functions of Eq. (16) can be regarded as the nodal counterpart of the modal basis functions: Jacobi polyfractonomials (Zayernouri & Karniadakis, 2013) and generalized Jacobi functions (Chen et al., 2016), which led to efficient Petrov–Galerkin spectral methods for fractional differential equations with appealing capability in fitting singularity of the underlying solutions (Zayernouri & Karniadakis, 2014; Chen et al., 2016).

4.2. Computation of ε-FPIMs

We present the general formulas for computing ε-FPIMs in the following two theorems, and omit the corresponding proofs since they are similar to that of FPIMs (Tang et al., 2015).

Theorem 11. *Let $\{\sigma_m^{\grave{\varepsilon}}, \omega_m^{\grave{\varepsilon}}\}_{m=1}^{\lceil N/2\rceil}$ be the set of JG points and quadrature weights with respect to the Jacobi weight function $\omega^{(\gamma-1,1-\gamma)}(\tau) = (1-\tau)^{\gamma-1}(1+\tau)^{1-\gamma}$. Then, the left ε-FPIMs of Eqs. (15a) and (17a) can be computed exactly as*

$${}_{-1}^{\tau}\boldsymbol{I}_{ki}^{\gamma_{\grave{\varepsilon}}} = \frac{\tau_k+1}{2\Gamma(\gamma)(\tau_i+1)^{1-\gamma}}\sum_{m=1}^{\lceil N/2\rceil}\omega_m^{\grave{\varepsilon}}\mathcal{L}_i(\sigma_m^{\grave{\varepsilon}};-1,\tau_k), \quad (k=1,2,\ldots,N+1,\ i=1,2,\ldots,N), \tag{18a}$$

$${}_{-1}^{\tau}\hat{\boldsymbol{I}}_{ki}^{\gamma_{\grave{\varepsilon}}} = \frac{\hat{\tau}_k+1}{2\Gamma(\gamma)(\hat{\tau}_i+1)^{1-\gamma}}\sum_{m=1}^{\lceil N/2\rceil}\omega_m^{\grave{\varepsilon}}\hat{\mathcal{L}}_i(\sigma_m^{\grave{\varepsilon}};-1,\hat{\tau}_k), \quad (k,i=1,2,\ldots,N). \tag{18b}$$

Theorem 12. *Let $\{\sigma_m^{\acute{\varepsilon}}, \omega_m^{\acute{\varepsilon}}\}_{m=1}^{\lceil N/2\rceil}$ be the set of JG points and quadrature weights with respect to the Jacobi weight function $\omega^{(1-\gamma,\gamma-1)}(\tau) = (1-\tau)^{1-\gamma}(1+\tau)^{\gamma-1}$. Then, the right ε-FPIMs of Eqs. (15b) and (17b) can be computed exactly as*

$${}_{\tau}^{1}\boldsymbol{I}_{ki}^{\gamma_{\acute{\varepsilon}}} = \frac{1-\tau_k}{2\Gamma(\gamma)(1-\tau_i)^{1-\gamma}}\sum_{m=1}^{\lceil N/2\rceil}\omega_m^{\acute{\varepsilon}}\mathcal{L}_i(\sigma_m^{\acute{\varepsilon}};\tau_k,1), \quad (k=0,1,\ldots,N,\ i=1,2,\ldots,N), \tag{19a}$$

$${}_{\tau}^{1}\check{\boldsymbol{I}}_{ki}^{\gamma_{\acute{\varepsilon}}} = \frac{1-\check{\tau}_k}{2\Gamma(\gamma)(1-\check{\tau}_i)^{1-\gamma}}\sum_{m=1}^{\lceil N/2\rceil}\omega_m^{\acute{\varepsilon}}\check{\mathcal{L}}_i(\sigma_m^{\acute{\varepsilon}};\check{\tau}_k,1), \quad (k,i=1,2,\ldots,N). \tag{19b}$$

Remark 13. Like FPIMs (see Tang et al., 2015, Remark 13), the last row of the left ε-FPIMs or the first row of the right ε-FPIMs with $\gamma=1$ also gives the quadrature weights to approximate the definite integral of a function on the interval $[-1,+1]$. Therefore, we will use them to approximate the cost functional of FOCPs as shown below.

5. Differential/integral fractional pseudospectral methods

In this section, the differential/integral scaled FOCP of Tang et al. (2015, Eqs. (8)–(11)/Eqs. (12)–(15)) is discretized using differential/integral fractional pseudospectral methods via FPDMs/ε-FPIMs. We omit the implementation of integral fractional pseudospectral methods since they can be derived directly from Tang et al. (2015, Section 5) by replacing FPIMs with ε-FPIMs.

5.1. Collocation at the JG points

First, the differential dynamic constraints of Tang et al. (2015, Eq. (9)) are discretized using collocation at the JG points $\{\tau_k\in(-1,+1)\}_{k=1}^N$ via the left FPDM as

$$\sum_{i=0}^{N}{}_{-1}^{\tau}\boldsymbol{D}_{ki}^{\gamma}\boldsymbol{x}_i = \left(\frac{t_f-t_0}{2}\right)^{\gamma}\boldsymbol{f}(\boldsymbol{x}_k,\boldsymbol{u}_k,\tau_k;t_0,t_f), \quad (k=1,2,\ldots,N), \tag{20}$$

where $\boldsymbol{x}_0\approx\boldsymbol{x}(-1)$, $\{\boldsymbol{x}_k\approx\boldsymbol{x}(\tau_k)\}_{k=1}^N$, $\{\boldsymbol{u}_k\approx\boldsymbol{u}(\tau_k)\}_{k=1}^N$, and ${}_{-1}^{\tau}\boldsymbol{D}^{\gamma}$ is the left FPDM for the JG points. Moreover, using the ε-FPIM version of Tang et al. (2015, Eq. (32)) with $k=N+1$ and taking Eq. (20) into account, we obtain $\boldsymbol{x}_{N+1}\approx\boldsymbol{x}(+1)$ as

$$\begin{aligned}
\boldsymbol{x}_{N+1} &= \boldsymbol{x}_0+\left(\frac{t_f-t_0}{2}\right)^{\gamma}\cdot\left(\sum_{i=1}^{N}{}_{-1}^{\tau}\boldsymbol{I}_{N+1,i}^{\gamma_{\grave{\varepsilon}}}\boldsymbol{f}(\boldsymbol{x}_i,\boldsymbol{u}_i,\tau_i;t_0,t_f)\right)\\
&= \boldsymbol{x}_0+\sum_{k=1}^{N}{}_{-1}^{\tau}\boldsymbol{I}_{N+1,k}^{\gamma_{\grave{\varepsilon}}}\cdot\left(\left(\frac{t_f-t_0}{2}\right)^{\gamma}\boldsymbol{f}(\boldsymbol{x}_k,\boldsymbol{u}_k,\tau_k;t_0,t_f)\right)\\
&= \boldsymbol{x}_0+\sum_{k=1}^{N}{}_{-1}^{\tau}\boldsymbol{I}_{N+1,k}^{\gamma_{\grave{\varepsilon}}}\cdot\left(\sum_{i=0}^{N}{}_{-1}^{\tau}\boldsymbol{D}_{ki}^{\gamma}\boldsymbol{x}_i\right)\\
&= \left(1+\sum_{k=1}^{N}\left({}_{-1}^{\tau}\boldsymbol{I}_{N+1,k}^{\gamma_{\grave{\varepsilon}}}\cdot{}_{-1}^{\tau}\boldsymbol{D}_{k0}^{\gamma}\right)\right)\boldsymbol{x}_0\\
&\quad+\sum_{i=1}^{N}\left(\sum_{k=1}^{N}\left({}_{-1}^{\tau}\boldsymbol{I}_{N+1,k}^{\gamma_{\grave{\varepsilon}}}\cdot{}_{-1}^{\tau}\boldsymbol{D}_{ki}^{\gamma}\right)\right)\boldsymbol{x}_i.
\end{aligned} \tag{21}$$

Next, the cost functional of Tang et al. (2015, Eq. (8)) is approximated using the quadrature as

$$J^N = \phi(\boldsymbol{x}_0,t_0,\boldsymbol{x}_{N+1},t_f)+\frac{t_f-t_0}{2}\cdot\left(\sum_{k=1}^{N}\omega_k^1 g(\boldsymbol{x}_k,\boldsymbol{u}_k,\tau_k;t_0,t_f)\right), \tag{22}$$

where the quadrature weights $\{\omega_k^1\}_{k=1}^N$ are given by

$$\omega_k^1 = {}_{-1}^{\tau}\boldsymbol{I}_{N+1,k}^{1_{\hat{\varepsilon}}}. \tag{23}$$

Furthermore, the path constraints of Tang et al. (2015, Eq. (10)) are evaluated at the JG points as

$$\boldsymbol{c}(\boldsymbol{x}_k, \boldsymbol{u}_k, \tau_k; t_0, t_f) \leq \boldsymbol{0}, \quad k = 1, 2, \ldots, N. \tag{24}$$

Finally, the boundary conditions of Tang et al. (2015, Eq. (11)) are approximated at the boundary points as

$$\boldsymbol{b}(\boldsymbol{x}_0, t_0, \boldsymbol{x}_{N+1}, t_f) = \boldsymbol{0}. \tag{25}$$

The cost function of Eq. (22) along with the algebraic constraints of Eqs. (20), (21), (24), and (25) defines an NLP which is the JG discretization of the differential scaled FOCP.

5.1.1. Collocation at the FJGR points

The differential dynamic constraints of Tang et al. (2015, Eq. (9)) are discretized using collocation at the FJGR points $\{\hat{\tau}_k \in (-1, +1]\}_{k=1}^N$ via the left FPDM as

$$\sum_{i=0}^{N} {}_{-1}^{\tau}\hat{\boldsymbol{D}}_{ki}^{\gamma}\hat{\boldsymbol{x}}_i = \left(\frac{t_f - t_0}{2}\right)^{\gamma} \boldsymbol{f}(\hat{\boldsymbol{x}}_k, \hat{\boldsymbol{u}}_k, \hat{\tau}_k; t_0, t_f), \quad (k = 1, 2, \ldots, N), \tag{26}$$

where $\hat{\boldsymbol{x}}_0 \approx \boldsymbol{x}(-1)$, $\{\hat{\boldsymbol{x}}_k \approx \boldsymbol{x}(\hat{\tau}_k)\}_{k=1}^N$, $\{\hat{\boldsymbol{u}}_k \approx \boldsymbol{u}(\hat{\tau}_k)\}_{k=1}^N$, and ${}_{-1}^{\tau}\hat{\boldsymbol{D}}^{\gamma}$ is the left FPDM for the FJGR points. Next, the cost functional of Tang et al. (2015, Eq. (8)) is approximated using the quadrature as

$$\hat{J}^N = \phi(\hat{\boldsymbol{x}}_0, t_0, \hat{\boldsymbol{x}}_N, t_f) + \frac{t_f - t_0}{2} \cdot \left(\sum_{k=1}^{N} \hat{\omega}_k^1 g(\hat{\boldsymbol{x}}_k, \hat{\boldsymbol{u}}_k, \hat{\tau}_k; t_0, t_f)\right), \tag{27}$$

where the quadrature weights $\{\hat{\omega}_k^1\}_{k=1}^N$ are given by

$$\hat{\omega}_k^1 = {}_{-1}^{\tau}\hat{\boldsymbol{I}}_{N,k}^{1_{\hat{\varepsilon}}}. \tag{28}$$

Furthermore, the path constraints of Tang et al. (2015, Eq. (10)) are evaluated at the FJGR points as

$$\boldsymbol{c}(\hat{\boldsymbol{x}}_k, \hat{\boldsymbol{u}}_k, \hat{\tau}_k; t_0, t_f) \leq \boldsymbol{0}, \quad k = 1, 2, \ldots, N. \tag{29}$$

Finally, the boundary conditions of Tang et al. (2015, Eq. (11)) are approximated at the boundary points as

$$\boldsymbol{b}(\hat{\boldsymbol{x}}_0, t_0, \hat{\boldsymbol{x}}_N, t_f) = \boldsymbol{0}. \tag{30}$$

Thus, the cost function of Eq. (27) along with the algebraic constraints of Eqs. (26), (29), and (30) defines an NLP which is the FJGR discretization of the differential scaled FOCP.

6. Equivalence between fractional pseudospectral methods

In this section, we prove the equivalence between the above fractional pseudospectral methods from the perspective of Caputo fractional Birkhoff interpolation by following Jiao, Wang, and Huang (2016, Section 4.1) where the Jacobi–Gauss–Lobatto (JGL) points are considered.

6.1. Caputo fractional Birkhoff interpolation

The Caputo fractional Birkhoff interpolation for the JG points of $\{\tau_i \in (-1, +1)\}_{i=1}^N$ with $-1 = \tau_0 < \tau_1 < \cdots < \tau_{N+1} = +1$ is stated as follows ($\gamma \in (0, 1]$):

$$\text{Find } h(\tau) \in \mathcal{P}_N \text{ such that } h(\tau_0) = q(\tau_0), \quad {}_{-1}^{C}\mathcal{D}_{\tau_i}^{\gamma} h(\tau) = {}_{-1}^{C}\mathcal{D}_{\tau_i}^{\gamma} q(\tau), \quad i = 1, 2, \ldots, N, \tag{31}$$

where $q(\tau) \in AC[-1, +1]$ is the given interpolated function. It can be readily verified that the above fractional Birkhoff interpolation is unique and the interpolant $h(\tau)$ can be expressed as

$$h(\tau) = q(\tau_0) \cdot \mathcal{B}_0^{\star}(\tau) + \sum_{i=1}^{N} {}_{-1}^{C}\mathcal{D}_{\tau_i}^{\gamma} q(\tau) \cdot \mathcal{B}_i^{\star}(\tau), \tag{32}$$

where $\{\mathcal{B}_i^{\star}(\tau) \in \mathcal{P}_N\}_{i=0}^N$ are the Birkhoff interpolating polynomials associated with the interpolating points $\{\tau_i\}_{i=0}^N$, which are the counterpart of the Lagrange interpolating polynomials $\{\mathcal{L}_i^{\star}(\tau)\}_{i=0}^N$. It follows from Eqs. (31) and (32) that

$$\mathcal{B}_0^{\star}(\tau_0) = 1, \quad \mathcal{B}_i^{\star}(\tau_0) = 0, \quad i = 1, 2, \ldots, N, \tag{33a}$$

$${}_{-1}^{C}\mathcal{D}_{\tau_k}^{\gamma}\mathcal{B}_0^{\star}(\tau) = 0, \quad {}_{-1}^{C}\mathcal{D}_{\tau_k}^{\gamma}\mathcal{B}_i^{\star}(\tau) = \delta_{ki} = \mathcal{L}_i^{\hat{\varepsilon}}(\tau_k), \quad (k, i = 1, 2, \ldots, N), \tag{33b}$$

where the last equality of Eq. (33b) results from the Kronecker property of the weighted Lagrange interpolating function of Eq. (16a). It follows from Jiao et al. (2016, Lemma 3.1) that

$${}_{-1}^{C}\mathcal{D}_{\tau}^{\gamma}\mathcal{B}_i^{\star}(\tau) \in \grave{\mathcal{Q}}_{N-1}^{1-\gamma}, \quad i = 1, 2, \ldots, N, \tag{34}$$

where $\grave{\mathcal{Q}}_N^{\nu} \triangleq \{(\tau + 1)^{\nu} p(\tau) : \forall\, \nu \in [0, 1),\ p(\tau) \in \mathcal{P}_N\}$. Using Eqs. (34) and (33b) along with the fact that $\{\mathcal{L}_i^{\hat{\varepsilon}}(\tau) \in \grave{\mathcal{Q}}_{N-1}^{1-\gamma}\}_{i=1}^N$, we have

$${}_{-1}^{C}\mathcal{D}_{\tau}^{\gamma}\mathcal{B}_i^{\star}(\tau) = \mathcal{L}_i^{\hat{\varepsilon}}(\tau), \quad i = 1, 2, \ldots, N. \tag{35}$$

Applying the operator ${}_{-1}\mathcal{I}_{\tau}^{\gamma}(\cdot)$ to Eq. (35) and taking account of Eq. (33a) yield ($\gamma \in (0, 1]$)

$$\mathcal{B}_i^{\star}(\tau) = \mathcal{B}_i^{\star}(-1) + {}_{-1}\mathcal{I}_{\tau}^{\gamma}\mathcal{L}_i^{\hat{\varepsilon}}(\tau) = {}_{-1}\mathcal{I}_{\tau}^{\gamma}\mathcal{L}_i^{\hat{\varepsilon}}(\tau), \quad i = 1, 2, \ldots, N. \tag{36}$$

Similarly, recalling that $\mathcal{B}_0^{\star}(\tau_0) = 1$, $\{{}_{-1}^{C}\mathcal{D}_{\tau_k}^{\gamma}\mathcal{B}_0^{\star}(\tau) = 0\}_{k=1}^N$, and ${}_{-1}^{C}\mathcal{D}_{\tau}^{\gamma}\mathcal{B}_0^{\star}(\tau) \in \grave{\mathcal{Q}}_{N-1}^{1-\gamma}$ yields

$$\mathcal{B}_0^{\star}(\tau_k) = 1, \quad k = 0, 1, \ldots, N. \tag{37}$$

Remark 14. Although we focus on the Caputo fractional Birkhoff interpolation for the JG points, the same idea can be extended to the FJGR points straightforwardly. Moreover, the classical Birkhoff interpolation (Tang et al., 2016) can be viewed as a special case of the Caputo fractional Birkhoff interpolation with $\gamma = 1$.

6.2. Equivalence proof using Caputo fractional Birkhoff interpolation

Now, the equivalence is summarized in the following theorem.

Theorem 15. *Let ${}_{-1}^{\tau}\boldsymbol{D}_{:,1:N}^{\gamma}$ be the matrix obtained by deleting the first column of ${}_{-1}^{\tau}\boldsymbol{D}^{\gamma}$, and ${}_{-1}^{\tau}\boldsymbol{I}_{1:N,:}^{\gamma_{\hat{\varepsilon}}}$ be the matrix obtained by deleting the last row of ${}_{-1}^{\tau}\boldsymbol{I}^{\gamma_{\hat{\varepsilon}}}$, then ${}_{-1}^{\tau}\boldsymbol{D}_{:,1:N}^{\gamma} \times {}_{-1}^{\tau}\boldsymbol{I}_{1:N,:}^{\gamma_{\hat{\varepsilon}}} = \boldsymbol{E}_N$ where $\boldsymbol{E}_N$ denotes the $N \times N$ identity matrix. Similarly, let ${}_{-1}^{\tau}\hat{\boldsymbol{D}}_{:,1:N}^{\gamma}$ be the matrix obtained by deleting the first column of ${}_{-1}^{\tau}\hat{\boldsymbol{D}}^{\gamma}$, then ${}_{-1}^{\tau}\hat{\boldsymbol{D}}_{:,1:N}^{\gamma} \times {}_{-1}^{\tau}\hat{\boldsymbol{I}}^{\gamma_{\hat{\varepsilon}}} = \boldsymbol{E}_N$.*

Proof. For any $p(\tau) \in \mathcal{P}_N$, we have

$$p(\tau) = \sum_{i=0}^{N} \mathcal{L}_i^{\star}(\tau) \cdot p(\tau_i). \tag{38}$$

Substituting $\{p(\tau) = \mathcal{B}_j^\star(\tau) \in \mathcal{P}_N\}_{j=1}^N$ into Eq. (38) and taking Eq. (33a) into account yield

$$\mathcal{B}_j^\star(\tau) = \sum_{i=0}^{N} \mathcal{L}_i^\star(\tau) \cdot \mathcal{B}_j^\star(\tau_i) = \sum_{i=1}^{N} \mathcal{L}_i^\star(\tau) \cdot \mathcal{B}_j^\star(\tau_i), \quad j = 1, 2, \ldots, N. \tag{39}$$

Moreover, it follows from Eqs. (36) and (15a) that

$$\mathcal{B}_j^\star(\tau_i) = {}_{-1}^{\tau}\boldsymbol{I}_{ij}^{\gamma_\varepsilon}, \quad i, j = 1, 2, \ldots, N. \tag{40}$$

Substituting Eq. (40) into Eq. (39) yields

$$\mathcal{B}_j^\star(\tau) = \sum_{i=1}^{N} \mathcal{L}_i^\star(\tau) \cdot {}_{-1}^{\tau}\boldsymbol{I}_{ij}^{\gamma_\varepsilon}, \quad j = 1, 2, \ldots, N. \tag{41}$$

Applying the operator ${}_{-1}^{C}\mathcal{D}_\tau^\gamma(\cdot)$ to Eq. (41) and evaluating the resulting identity at $\{\tau = \tau_k\}_{k=1}^N$ lead to

$${}_{-1}^{C}\mathcal{D}_{\tau_k}^\gamma \mathcal{B}_j^\star(\tau) = \sum_{i=1}^{N} {}_{-1}^{C}\mathcal{D}_{\tau_k}^\gamma \mathcal{L}_i^\star(\tau) \cdot {}_{-1}^{\tau}\boldsymbol{I}_{ij}^{\gamma_\varepsilon}, \quad (k, j = 1, 2, \ldots, N). \tag{42}$$

Substituting Eqs. (33b) and (3a) into Eq. (42) yields

$$\delta_{kj} = \sum_{i=1}^{N} {}_{-1}^{\tau}\boldsymbol{D}_{ki}^{\gamma} \cdot {}_{-1}^{\tau}\boldsymbol{I}_{ij}^{\gamma_\varepsilon}, \quad k, j = 1, 2, \ldots, N. \tag{43}$$

This implies that

$$\boldsymbol{E}_N = {}_{-1}^{\tau}\boldsymbol{D}_{:,1:N}^{\gamma} \times {}_{-1}^{\tau}\boldsymbol{I}_{1:N,:}^{\gamma_\varepsilon}. \tag{44}$$

In the same way, ${}_{-1}^{\tau}\hat{\boldsymbol{D}}_{:,1:N}^{\gamma} \times {}_{-1}^{\tau}\hat{\boldsymbol{I}}^{\gamma_\varepsilon} = \boldsymbol{E}_N$ can be obtained. □

Remark 16. For the right FPDMs and ε-FPIMs, we have ${}_{\tau}^{1}\boldsymbol{D}_{:,1:N}^{\gamma} \times {}_{\tau}^{1}\boldsymbol{I}_{1:N,:}^{\gamma_\varepsilon} = \boldsymbol{E}_N$ and ${}_{\tau}^{1}\check{\boldsymbol{D}}_{:,1:N}^{\gamma} \times {}_{\tau}^{1}\check{\boldsymbol{I}}^{\gamma_\varepsilon} = \boldsymbol{E}_N$, where ${}_{\tau}^{1}\boldsymbol{D}_{:,1:N}^{\gamma}$ (resp. ${}_{\tau}^{1}\check{\boldsymbol{D}}_{:,1:N}^{\gamma}$) denotes the matrix obtained by deleting the last column of ${}_{\tau}^{1}\boldsymbol{D}^{\gamma}$ (resp. ${}_{\tau}^{1}\check{\boldsymbol{D}}^{\gamma}$) and ${}_{\tau}^{1}\boldsymbol{I}_{1:N,:}^{\gamma_\varepsilon}$ denotes the matrix obtained by deleting the first row of ${}_{\tau}^{1}\boldsymbol{I}^{\gamma_\varepsilon}$.

7. Some comments on fractional pseudospectral methods

In this section, we make some comments regarding the scopes and features of fractional pseudospectral methods.

Remark 17. Similar to FPIMs (see Tang et al., 2015, Remark 14), it is clear from Theorems 5, 6, 11, and 12 that both of FPDMs and ε-FPIMs can be computed efficiently and stably for millions of Jacobi-type points in an $\mathcal{O}(N^2)$ complexity.

Remark 18. It is easy to see that classical pseudospectral methods (Benson et al., 2006; Garg et al., 2010; Francolin et al., 2015) are special cases of the proposed fractional pseudospectral methods with collocation at the Legendre-type points and $\gamma = 1$.

Remark 19. The present work establishes a new unified framework for solving optimal control problems using pseudospectral methods, which can be viewed as the extension of existing frameworks (Garg et al., 2010; Tang et al., 2015).

Remark 20. Although differential and integral fractional pseudospectral methods are equivalent, the former has higher computational efficiency than the latter as the corresponding constraint Jacobians resulting from collocation are more easy to compute.

8. Examples

In this section, the proposed methods are applied to two benchmark FOCPs taken from the open literature. All computations were performed on a 3.6 GHz Intel Core i7 desktop with 16 GB of 1600 MHz DDR3 RAM running Windows Version 10 and MATLAB Version R2015b.

8.1. Example 1: linear time-varying problem

Consider the following linear time-varying FOCP (Lotfi, Dehghan, & Yousefi, 2011). Determine the state, $x(t) \in \mathbb{R}$, and the control, $u(t) \in \mathbb{R}$, on the time interval $t \in [0, 1]$ that minimize the cost functional

$$J = \frac{1}{2}\int_0^1 \left(x^2(t) + u^2(t)\right) \mathrm{d}t, \tag{45}$$

subject to the dynamic constraint ($\gamma \in (0, 1]$)

$${}_{0}^{C}\mathcal{D}_t^\gamma x(t) = tx(t) + u(t), \tag{46}$$

and the boundary condition

$$x(0) = 1. \tag{47}$$

The example was solved using the differential fractional pseudospectral scheme with collocation at the flipped Legendre–Gauss–Radau (FLGR) points and the NLP solver SNOPT (Gill et al., 2005) with optimality and feasibility tolerances of 10^{-10} and 2×10^{-10}, respectively. A linear initial guess was used for the state while a zero initial guess was used for the control. The solutions of state and control for $N = 30$ and $\gamma = 0.1, 0.3, 0.5, 0.7, 1.0$ are shown in Fig. 1 along with the solutions obtained using the direct scheme (Agrawal & Baleanu, 2007) with $h = 0.001$ (i.e., the number of equidistant nodes is 1001). It is seen that both the state and control solutions change more rapidly near the boundaries as γ is decreased. With regard to accuracy, it is clear from Table 1 that the pseudospectral scheme achieves smaller cost than the direct scheme (Agrawal & Baleanu, 2007) for various γ using only 30 FLGR points. Finally, the average execution times of 100 independent runs for the pseudospectral scheme and the direct scheme (Agrawal & Baleanu, 2007) are 0.42 s and 1.73 s, respectively.

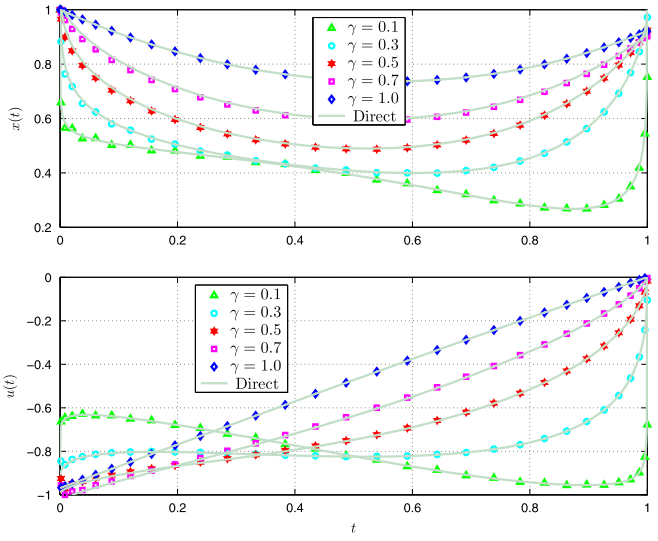

Fig. 1. Solution to Example 1 using direct scheme (Agrawal & Baleanu, 2007) and pseudospectral scheme.

8.2. Example 2: fractional bang–bang problem

Consider the following fractional bang–bang problem (Tricaud & Chen, 2010). Determine the state, $\boldsymbol{x}(t) \triangleq [x_1(t), x_2(t)]^T \in \mathbb{R}^2$, and the control, $u(t) \in [-2, 1]$, on the time interval $t \in [0, t_f]$ that minimize the cost functional

$$J = t_f, \tag{48}$$

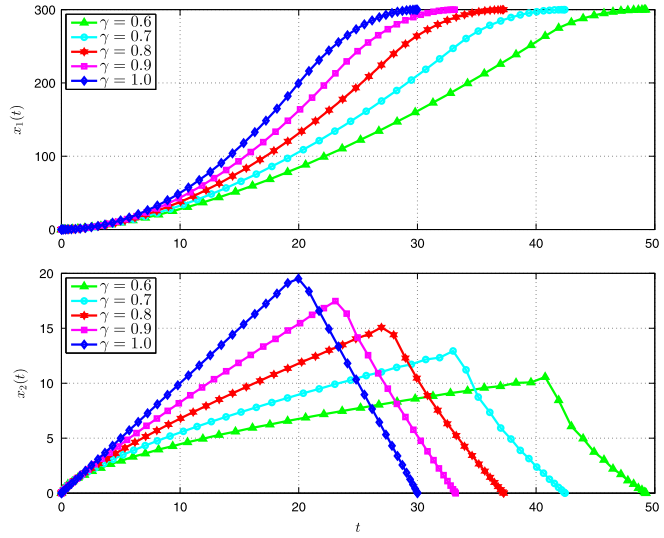

Fig. 2. State solution to Example 2 for $N = 50$ and $\gamma = 0.6, 0.7, 0.8, 0.9, 1.0$.

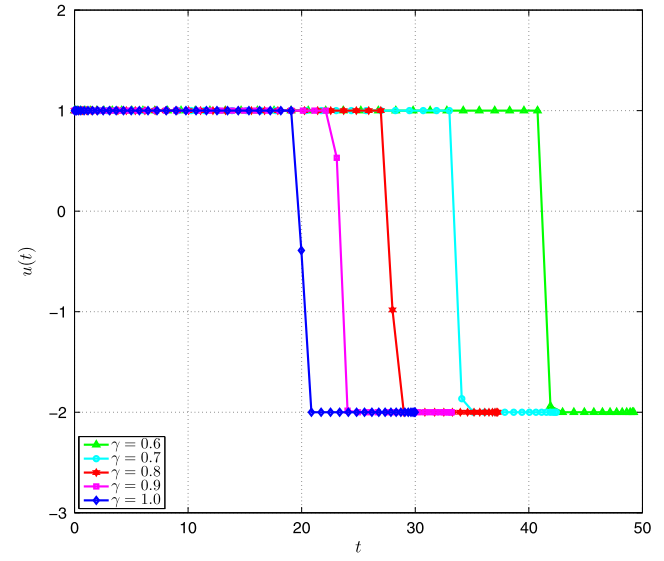

Fig. 3. Control solution to Example 2 for $N = 50$ and $\gamma = 0.6, 0.7, 0.8, 0.9, 1.0$.

Table 1
Optimal cost of Example 1 for direct scheme (Agrawal & Baleanu, 2007) and pseudospectral scheme.

γ	0.1	0.2	0.3	0.4	0.5
Direct	0.4173	0.4290	0.4354	0.4412	0.4488
Pseudospectral	0.4155	0.4270	0.4325	0.4369	0.4425
γ	0.6	0.7	0.8	0.9	1.0
Direct	0.4582	0.4682	0.4766	0.4814	0.4854
Pseudospectral	0.4497	0.4581	0.4671	0.4759	0.4843

Table 2
Optimal cost of Example 2.

γ	0.1	0.2	0.3	0.4	0.5
t_f	186.2077	125.7254	91.7457	71.9079	58.5884
γ	0.6	0.7	0.8	0.9	1.0
t_f	49.2539	42.4375	37.2741	33.2272	30.0098

subject to the dynamic constraints ($\gamma \in (0, 1]$)

$$\dot{x}_1(t) = x_2(t), \tag{49a}$$

$${}_0^C\mathcal{D}_t^{\gamma} x_2(t) = u(t), \tag{49b}$$

and the boundary conditions

$$\boldsymbol{x}(0) = \boldsymbol{0}, \qquad \boldsymbol{x}(t_f) = [300, 0]^T. \tag{50}$$

For this problem we have the exact solution in the only case of $\gamma = 1$ as

$$t_f^* = 30, \tag{51a}$$

$$x_1^*(t) = \begin{cases} t^2/2, & t \in [0, 20) \\ -t^2 + 60t - 600, & t \in [20, 30], \end{cases} \tag{51b}$$

$$x_2^*(t) = \begin{cases} t, & t \in [0, 20) \\ -2t + 60, & t \in [20, 30], \end{cases} \tag{51c}$$

$$u^*(t) = \begin{cases} 1, & t \in [0, 20) \\ -2, & t \in [20, 30]. \end{cases} \tag{51d}$$

The example was solved using the differential fractional pseudospectral scheme with collocation at the JG points of $(\alpha, \beta) = (-0.25, -0.75)$ and the NLP solver SNOPT (Gill et al., 2005) with default optimality and feasibility tolerances of 10^{-6} and 2×10^{-6}, respectively. The initial guess used for the state and control was a linear interpolation over the exact initial and final values. The state and control solutions are shown, respectively, in Figs. 2 and 3 for $N = 50$ and $\gamma = 0.6, 0.7, 0.8, 0.9, 1.0$. As can be seen, the numerical solution for $\gamma = 1$ is in excellent agreement with the exact solution of Eq. (51), and t_f decreases as γ is increased which is consistent with Table 2. Moreover, the bang–bang control is observed and this agrees well with our expectation.

9. Conclusions

This paper provided differential and integral fractional pseudospectral methods with equivalence for solving FOCPs, and proved the equivalence from the distinctive perspective of Caputo fractional Birkhoff interpolation. Moreover, this paper provided exact, efficient, and stable approaches for computing the associated fractional pseudospectral differentiation/integration matrices. The performance of the proposed methods was demonstrated on two benchmark FOCPs including a fractional bang–bang problem. Costate mapping principle for fractional pseudospectral methods and general optimality conditions for FOCPs should be investigated for future work.

Acknowledgments

The authors would like to express their gratitude to the associate editor and the anonymous reviewers for their constructive comments, which shaped the paper into its final form.

The work of X. Tang was partially supported by the Fundamental Research Funds for the Central Universities (Grant No. 3102016ZY003). The work of Y. Shi was partially supported by the Natural Sciences and Engineering Research Council of Canada (NSERC RGPIN-2016-05386), and the National Natural Science

Foundation of China (Grant No. 61473116). The work of L.-L. Wang was partially supported by Singapore MOE AcRF Tier 1 Grants (RG15/12 and RG27/15), and Singapore MOE AcRF Tier 2 Grant (MOE 2013-T2-1-095, ARC 44/13).

Appendix. Proof of Eq. (14b)

Proof. Differentiating both sides of Eq. (6b) with respect to τ and evaluating the resulting identity at $\{\tau = \tau_r\}_{r=1}^{N}$ yield

$$\dot{\mathcal{L}}_i^{\dagger}(\tau_r) = -\frac{\mathcal{L}_i(\tau_r) - (\tau_{N+1} - \tau_r)\dot{\mathcal{L}}_i(\tau_r)}{\tau_{N+1} - \tau_i}, \quad (r, i = 1, 2, \ldots, N). \tag{A.1}$$

Combining Eqs. (14a), (A.1) and (10a), and taking account of $\mathcal{L}_i(\tau_r) = \delta_{ri}$ lead to

$${}_{\tau}^{1}\boldsymbol{D}_{ri}^{1} = \frac{\delta_{ri} - (\tau_{N+1} - \tau_r)\boldsymbol{D}_{ri}}{\tau_{N+1} - \tau_i}, \quad r, i = 1, 2, \ldots, N, \tag{A.2}$$

which is the first identity of Eq. (14b). In a manner similar to the first identity of Eq. (9b), the second identity of Eq. (14b) can be obtained. □

References

Agrawal, O. P. (2004). A general formulation and solution scheme for fractional optimal control problems. *Nonlinear Dynamics*, *38*(1–4), 323–337.

Agrawal, O. P., & Baleanu, D. (2007). A Hamiltonian formulation and a direct numerical scheme for fractional optimal control problems. *Journal of Vibration and Control*, *13*(9–10), 1269–1281.

Benson, D. A., Huntington, G. T., Thorvaldsen, T. P., & Rao, A. V. (2006). Direct trajectory optimization and costate estimation via an orthogonal collocation method. *Journal of Guidance, Control, and Dynamics*, *29*(6), 1435–1440.

Berrut, J.-P., & Trefethen, L. N. (2004). Barycentric Lagrange interpolation. *SIAM Review*, *46*(3), 501–517.

Biegler, L. T., & Zavala, V. M. (2009). Large-scale nonlinear programming using IPOPT: An integrating framework for enterprise-wide dynamic optimization. *Computers and Chemical Engineering*, *33*(3), 575–582.

Chen, S., Shen, J., & Wang, L.-L. (2016). Generalized Jacobi functions and their applications to fractional differential equations. *Mathematics of Computation*, *85*(300), 1603–1638.

Elnagar, G., Kazemi, M. A., & Razzaghi, M. (1995). The pseudospectral Legendre method for discretizing optimal control problems. *IEEE Transactions on Automatic Control*, *40*(10), 1793–1796.

Fahroo, F., & Ross, I. M. (2001). Costate estimation by a Legendre pseudospectral method. *Journal of Guidance, Control, and Dynamics*, *24*(2), 270–277.

Francolin, C. C., Benson, D. A., Hager, W. W., & Rao, A. V. (2015). Costate approximation in optimal control using integral Gaussian quadrature orthogonal collocation methods. *Optimal Control Applications & Methods*, *36*(4), 381–397.

Garg, D., Patterson, M. A., Francolin, C., Darby, C. L., Huntington, G. T., Hager, W. W., et al. (2011). Direct trajectory optimization and costate estimation of finite-horizon and infinite-horizon optimal control problems using a Radau pseudospectral method. *Computational Optimization and Applications*, *49*(2), 335–358.

Garg, D., Patterson, M., Hager, W. W., Rao, A. V., Benson, D. A., & Huntington, G. T. (2010). A unified framework for the numerical solution of optimal control problems using pseudospectral methods. *Automatica*, *46*(11), 1843–1851.

Gill, P. E., Murray, W., & Saunders, M. A. (2005). SNOPT: An SQP algorithm for large-scale constrained optimization. *SIAM Review*, *47*(1), 99–131.

Huntington, G. T. (2007). *Advancement and analysis of a Gauss pseudospectral transcription for optimal control problems* (Ph.D. thesis), Massachusetts Institute of Technology.

Jiao, Y., Wang, L.-L., & Huang, C. (2016). Well-conditioned fractional collocation methods using fractional Birkhoff interpolation basis. *Journal of Computational Physics*, *305*, 1–28.

Kilbas, A. A., Srivastava, H. M., & Trujillo, J. J. (2006). *Theory and applications of fractional differential equations* (1st ed.). Amsterdam, Netherlands: Elsevier Science.

Lotfi, A., Dehghan, M., & Yousefi, S. A. (2011). A numerical technique for solving fractional optimal control problems. *Computers and Mathematics with Applications*, *62*(3), 1055–1067.

Oldham, K. B., & Spanier, J. (2006). *The fractional calculus: Theory and applications of differentiation and integration to arbitrary order* (1st ed.). New York: Dover Publications.

Sabatier, J., Agrawal, O. P., & Tenreiro Machado, J. A. (2007). *Advances in fractional calculus: Theoretical developments and applications in physics and engineering* (1st ed.). New York: Springer-Verlag.

Tang, X., Liu, Z., & Hu, Y. (2016). New results on pseudospectral methods for optimal control. *Automatica*, *65*, 160–163.

Tang, X., Liu, Z., & Wang, X. (2015). Integral fractional pseudospectral methods for solving fractional optimal control problems. *Automatica*, *62*, 304–311.

Tricaud, C., & Chen, Y. Q. (2010). An approximate method for numerically solving fractional order optimal control problems of general form. *Computers and Mathematics with Applications*, *59*(5), 1644–1655.

Wang, H., Huybrechs, D., & Vandewalle, S. (2014). Explicit barycentric weights for polynomial interpolation in the roots or extrema of classical orthogonal polynomials. *Mathematics of Computation*, *83*(290), 2893–2914.

Weideman, J. A. C., & Reddy, S. C. (2000). A MATLAB differentiation matrix suite. *ACM Transactions on Mathematical Software*, *26*(4), 465–519.

Zayernouri, M., & Karniadakis, G. E. (2013). Fractional Sturm–Liouville eigen-problems: Theory and numerical approximation. *Journal of Computational Physics*, *252*, 495–517.

Zayernouri, M., & Karniadakis, G. E. (2014). Exponentially accurate spectral and spectral element methods for fractional ODEs. *Journal of Computational Physics*, *257*, 460–480.

Xiaojun Tang received the B.S., M.S., and Ph.D. degrees from Northwestern Polytechnical University, China, in 2002, 2005, and 2010, respectively. He is currently an Associate Professor with the School of Aeronautics, Northwestern Polytechnical University, China. He was a visiting scholar with the Applied Control and Information Processing Lab (ACIPL), University of Victoria, Canada, from September 2015 to September 2016. His research interests include optimal control, state estimation, and pseudospectral methods.

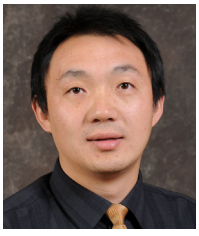

Yang Shi received the Ph.D. degree in electrical and computer engineering from the University of Alberta, Edmonton, AB, Canada, in 2005. Now he is a Professor in the Department of Mechanical Engineering, University of Victoria, Victoria, British Columbia, Canada. His current research interests include networked and distributed control systems, model predictive control, system identification, mechatronics, autonomous vehicles, cyber-physical systems, and energy system applications.

Dr. Shi received the University of Saskatchewan Student Union Teaching Excellence Award in 2007, the Faculty of Engineering Teaching Excellence Award at the University of Victoria in 2012. He received the 2017 IEEEE TFS Outstanding Paper award, the Craigdarroch Silver Medal for Excellence in Research of the University of Victoria in 2015, and the JSPS Invitation Fellowship (short-term) in 2013. He serves as Associate Editor for IEEE/ASME Trans. Mechatronics, IEEE Trans. Industrial Electronics, IEEE Trans. Control Systems Technology, IEEE Trans. Cybernetics, ASME Journal of Dynamic Systems, Measurement, and Control. He is currently a Fellow of IEEE, ASME and CSME, and a registered Professional Engineer in British Columbia, Canada.

Li-Lian Wang received his Ph.D. degree in Computational Mathematics from Shanghai University, China in 2000. He is currently an Associate Professor with the Division of Mathematical Sciences in the School of Physical and Mathematical Sciences of Nanyang Technological University, Singapore. His research interests include numerical methods for partial differential equations, computational electromagnetics and image processing based on variational techniques and partial differential equations.